Available online at www.sciencedirect.com
SCIENCE DIRECT®
Chemical Engineering and Processing 43 (2004) 161–167
Chemical Engineering and Processing
www.elsevier.com/locate/cep

# Eutectic freeze crystallization in a new apparatus: the cooled disk column crystallizer

Frank van der Ham, Marcelo Martins Seckler, Geert Jan Witkamp*

*Laboratory for Process Equipment, Delft University of Technology, Leeghwaterstraat 44, 2628 CA Delft, Netherlands*

Received 21 June 2002; received in revised form 21 February 2003; accepted 21 February 2003

**Abstract**

Eutectic freeze crystallization (EFC) is a technique for simultaneous crystallization of ice and salt that is energetically more efficient than conventional evaporative crystallization. In this paper, a new type of crystallizer is introduced for simultaneously conducting EFC and separating the ice from the salt crystals, the cooled disk column crystallizer (CDCC). Crystallization is achieved by indirect cooling with wiped disks and separation by means of gravity. The liquid feed stream enters the column at the center, ice leaves the column at the top and salt is discharged at the bottom. The heat flux from bulk fluid to disk in a 14 l CDCC using $CuSO_4$–water as a model system (eutectic temperature −1.6 °C) was 1.9 kW $m^{-2}$ for a temperature difference between disk and bulk of 4.5 K. The $CuSO_4 \cdot 5H_2O$ crystals formed were well faceted with an average size of 200 μm. Ice crystals were disk shaped with an average size 150 μm. Both ice and salt crystals were easily filtered. The impurity level in the ice crystals was below 100 ppm Cu.


*Keywords:* Eutectic freeze crystallization; Ice; Copper sulfate pentahydrate; Cooled disk column crystallizer

## 1. Introduction

Eutectic freeze crystallization (EFC) is potentially a technique to separate inorganic aqueous solutions into pure ice and solidified solutes by means of freezing at the eutectic point [1–3]. Compared with the conventional techniques of evaporative and cooling crystallization, the advantages of EFC are, respectively, the low energy requirement and the theoretical possibility of complete conversion of feed into water and solidified solutes [4]. A continuous EFC system based on direct cooling in a mixed crystallizer followed by salt–ice separation has been developed to bench scale [2,3]. However, this method generally leads to fine ice and salt crystals, which requires complex and costly solid–liquid separation systems. Besides, coolant separation and recompression have to be dealt with. Since the density difference between ice and salt is usually high, it is possible to conduct EFC and separation of the solid phases in one piece of equipment. If additionally heat removal is made indirectly, the ice and salt crystals obtained are easier to separate than those obtained by the direct method. In this work, a new type of EFC equipment is thus described, capable of crystallizing and separating ice and salt from an aqueous feed stream, the cooled disk column crystallizer (CDCC). The crystallizer performance is assessed in terms of the heat transfer rate, the quality of the ice and salt crystals formed (purity, shape, size) and the yield.

## 2. The cooled disk column crystallizer

Fig. 1 shows the phase diagram of a binary aqueous system at low temperature. Cooling of a solution originally in the state A results in ice formation at point B. Further cooling causes additional ice formation, thereby increasing the solute concentration in the liquid along the path B→C until the eutectic point D is reached. Additional cooling results in the formation of both ice and salt.

In a ternary system, there are two eutectic lines, corresponding to coexistence of ice with each of the two possible solid phases, as well as one ternary eutectic point where the solution exists with three solid phases. For systems with more components, similar eutectic regions exist. EFC can in principle be operated either near the true eutectic point or any eutectic regions with two solid phases in equilibrium.

* Corresponding author. Tel.: +31-15-278-6678; fax: +31-15-278-6975.
*E-mail address:* g.j.witkamp@wbmt.tudelft.nl (G.J. Witkamp).

0255-2701/$ – see front matter © 2003 Elsevier B.V. All rights reserved.
doi:10.1016/S0255-2701(03)00018-7

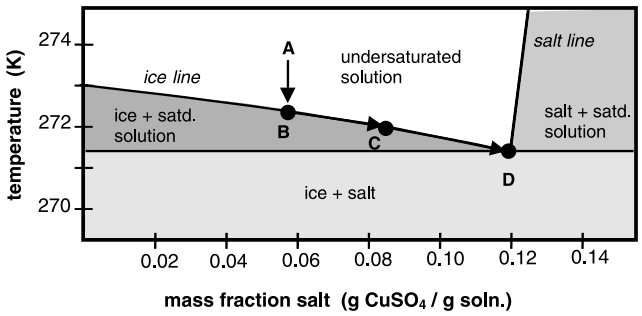


Fig. 1. Phase diagram of the water–copper sulfate pentahydrate system. Point D is the eutectic point.

In the CDCC, not only crystallization of ice and salt takes place, but also their gravitational separation. The main unit operations involved in the EFC of a binary system are depicted in Fig. 2. Ice crystals that leave the crystallizer through the top are subsequently fed to a wash column. The adhering liquid is removed from the ice crystals by washing and the ice crystals are melted. Part of the melted ice is used in the wash column as wash fluid. The wash liquid eventually solidifies on the ice crystals, thereby being completely recovered as product [5]. The salt crystals are discharged from the bottom of the crystallizer and filtered. The adhering liquid from the ice and salt crystals is recycled back to the crystallizer. The products are pure water and pure salt crystals.

Fig. 3 shows a schematic representation of the CDCC. Cooling is provided by means of disks that are wiped to prevent scaling and to improve heat transfer. The feed streams enter the crystallizer at the center of the column. Liquid as well as solids are axially transported through orifices in the cooling disks.

The heat flow $\phi_H$ (kW) from the bulk fluid to the cooling disk can be described by Newton's law, shown in Eq. (1), where $A_{cool}$ ($m^2$) is the surface of the cooling disk; $\bar{T}_{bulk}$ and $\bar{T}_{disk}$ (K) are the average temperatures in the bulk of the solution and on the cooling disk; $\alpha$ is the heat transfer coefficient (kW $K^{-1}$ $m^{-2}$). The heat flux $\phi''_H$ (kW $m^{-2}$) is defined by Eq. (2). Industrial crystallizers with a similar cooling mechanism are reported to operate with heat fluxes in the range of 1–2 kW $m^{-2}$ [6].

$$\phi_H = A_{cool}\alpha(\bar{T}_{bulk} - \bar{T}_{disk}) \quad (1)$$

$$\phi''_H = \phi_H / A_{cool} \quad (2)$$

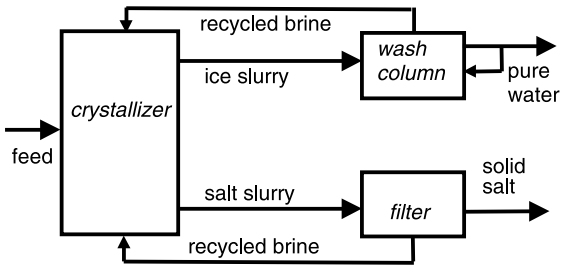


Fig. 2. Basic process steps of EFC.

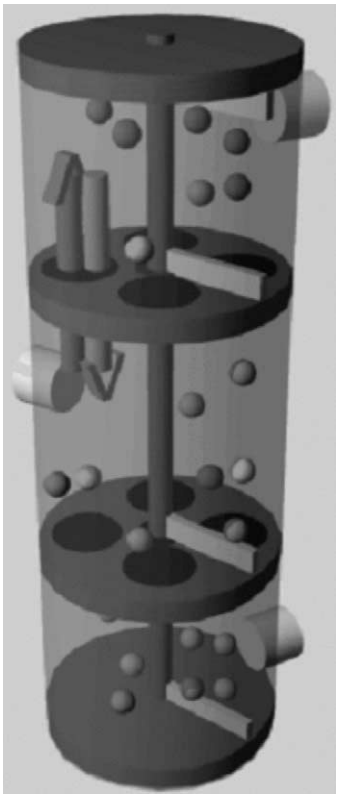

Fig. 3. Schematic representation of the CDCC.

For the system Cu–$SO_4$–$H_2O$, copper sulfate pentahydrate ($CuSO_4 \cdot 5H_2O$) is formed. This system can be described by a $CuSO_4$ balance (Eq. (3)), a water balance (Eq. (4)), a heat balance for the crystallizer (Eq. (5)) and a heat balance for the coolant (Eq. (6)). The flows in Eqs. (3)–(6) are indicated in Fig. 4. It is assumed that salt and ice crystals are pure. As a small supercooling within the range of 0.1–0.4 K is established, it is neglected: the crystallizer is assumed to operate at the eutectic temperature.

$$x_f \dot{m}_f = x_{top}\dot{m}_{liq,top} + x_{bot}\dot{m}_{liq,bot} + x_{s,anh}\dot{m}_{salt} \quad (3)$$

$$(1 - x_f)\dot{m}_f = (1 - x_{top})\dot{m}_{liq,top} + (1 - x_{bot})\dot{m}_{liq,bot} + (1 - x_{s,anh})\dot{m}_{salt} + \dot{m}_{ice} \quad (4)$$

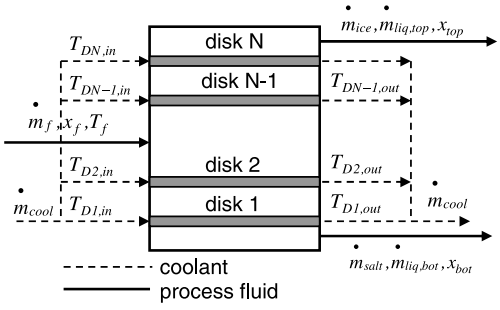


Fig. 4. Flow diagram for a CDCC.

$$\phi_H = \dot{m}_f C_{p,feed}(T_f - T_{eutec}) + \dot{m}_{ice}\Delta H_{crys,ice} + \dot{m}_{salt}\Delta H_{crys,salt} \quad (5)$$

$$\phi_H = \frac{\dot{m}_{cool}}{N} C_{p,cool} \sum_{i=1}^{N} (T_{Di,out} - T_{Di,in}) \quad (6)$$

The eutectic temperature and composition are, respectively, $T_{eutec}$ 271.55 K and $x_{eutec}$ 0.119 kg anhydrous salt $kg^{-1}$ solution. The heats of crystallization of ice and copper sulfate at the eutectic temperature and composition are, respectively, $\Delta H_{crys,ice} = 334$ kJ $kg^{-1}$ and $\Delta H_{crys,salt} = 48$ kJ $kg^{-1}$. The quantity $x_{s,anh}$ is the mass $CuSO_4$ per unit mass $CuSO_4 \cdot 5H_2O$. N is the number of cooling disks.

Eq. (6) and measurement of the coolant flow and temperatures provide the heat flow $\phi_H$. Alternatively, $\phi_H$ can be obtained from measured process flows and compositions with Eqs. (3)–(5). The heat flux is calculated from $\phi_H$ and the cooling surface area through Eq. (2). The error in the heat transfer measurement $\varepsilon(\phi_H)$ depends on the error of the temperature sensors $\varepsilon(T)$. For a CDCC with two cooling disks it holds that:

$$\varepsilon(\phi_H) = \frac{\dot{m}_{cool}}{2} C_{p,cool} 4\varepsilon(T) \quad (7)$$

$$\varepsilon(\phi''_H) = \frac{\varepsilon(\phi_H)}{A_{cool}} \quad (8)$$

## 3. Experimental

Fig. 5 schematically shows the experimental setup. The continuously operated crystallizer is fed with a copper sulfate solution from a 100 l storage vessel (indicated "store" in Fig. 5). Although EFC can be applied to solutions of any concentration, for this study a feed containing 0.145 kg anhydrous salt $kg^{-1}$ solution is used. The feed solution is pumped to a pre-cooling heat exchanger ("htxr"). The bottom flow is pumped to the product vessel ("product"). Ice slurry overflows through the top to the same vessel. The 14-l CDCC crystallizer (Fig. 6) consists of three compartments separated by two wiped, perforated, cooling disks (total cooling surface area $A_{cool}$ 0.03575 $m^2$). The compartments are made of transparent material to allow visual observation of the process. The CDCC is cooled with methanol (heat capacity $C_{p,cool}$ 2.5344 kJ $kg^{-1}$ °$C^{-1}$) that circulates through a thermostatic unit with a flow rate $\dot{m}_{cool}$ of 0.104 kg $s^{-1}$.

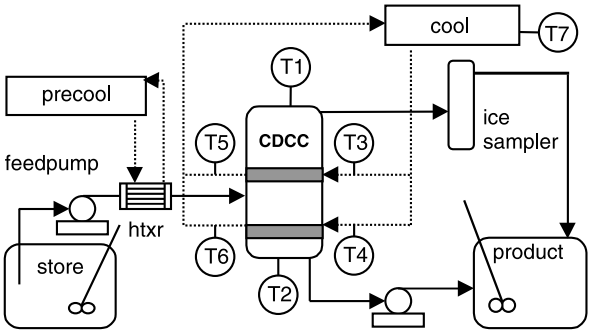


Fig. 5. Experimental set-up. Temperature sensors: T1, T2, suspension; T3, T4, inlet cooling fluid; T5, T6, outlet cooling fluid; T7, thermostatic bath.

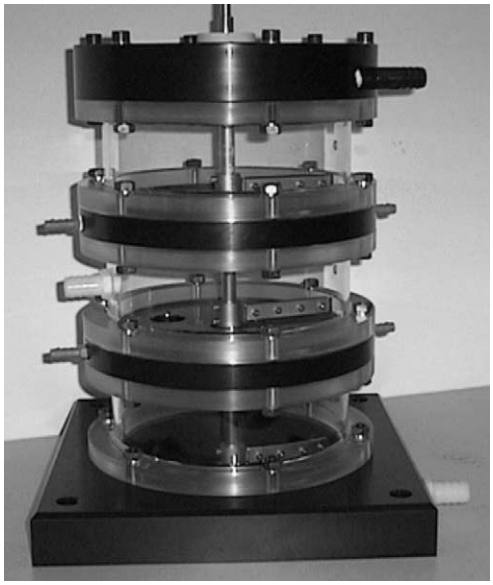

Fig. 6. Cooled disk column crystallizer.

The residence time $\tau$ was defined as the crystallizer volume divided by the volumetric flow of the feed. Defined in this way, $\tau$ approaches the residence time that would be relevant in the technical case when there are reflux streams from the two separators, i.e. taking the crystallizer and reflux systems as control volumes and neglecting the volumes of these reflux systems. The feed flow was adjusted to give the residence times between 50 and 120 min.

The ratio between the mass flow rates at the top and bottom outlets of the CDCC ($R$) was such that allowed technical production of ice and salt without excessive scaling and blockage of outlet ports. The operating conditions are shown in Table 1.

Table 1
Experimental conditions

| Exp. | $T_D$ (K) | $\tau$ (min) | $R$ (−) |
|---|---|---|---|
| 1 | 266.9 | 120 | * |
| 2 | 267.1 | 120 | * |
| 3 | 266.3 | 120 | * |
| 4 | 266.4 | 93 | 1.7 |
| 5 | 266.4 | 129 | 0.8 |
| 6 | 266.4 | 109 | 0.9 |
| 7 | 267.5 | 51 | 1.2 |
| 8 | 266.2 | 59 | 1.5 |
| 9 | 266.7 | 59 | 1.3 |
| 10 | 266.2 | 60 | 1.0 |
| 11 | 266.5 | 53 | 1.1 |
| 12 | 267.2 | 54 | 1.2 |

**$T_D$** is the temperature of the cooling medium; $\tau$ is the residence time; **R** is the mass flow ratio between bottom and top outlets of the CDCC; fields marked with * indicate no measurement made.

Seven temperature sensors are used, as indicated in Fig. 5, with measurement errors $\varepsilon(T)$ of 0.05 K. Flow rates of the overflow and underflow streams are determined from the mass collected in an insulated flask after a known a period of time. Corresponding solids concentrations are determined by filtration of the samples just referred and weighing the filtrate. Liquid compositions are determined from density measurements of the filtrates with a picnometer.

The concentration of copper incorporated in the ice crystals is determined from the following procedure. The ice slurry leaving the CDCC is collected by gravity in a glass column (see Fig. 5, "ice sampler"). At the center of the column, liquid is removed by means of a pump. About 300 ml of the ice bed formed at the top of the column is scooped into a thermally isolated flask and transported to a cold room set at 273 K. In this room the ice crystals are first vacuum-filtered on a glass filter. The filter cake is suspended (washed) with distilled water at 273 K. Vacuum filtration is applied again to remove the wash water. This procedure of washing and filtration is repeated several times. The washed ice crystals are melted and analyzed for the concentration of copper with inductively coupled plasma spectrometry. Ice crystals are directly collected from the top of the column and transported to the cold room for optical microscopic analysis. Salt crystals obtained by filtration of the bottom outlet flow of the CDCC are analyzed by optical microscopy.

## 4. Results and discussion

### 4.1. Operation of the CDCC

In order to promote ice and salt crystallization, a relatively low temperature of the cooling fluid is required. A too low temperature, however, promotes excessive scaling that hampers heat transfer. For a chosen feed rate and temperature of the cooling bath, the bottom flow rate is adjusted in such a way that the top and bottom flow can be easily pumped. These technical restrictions limited the spectrum of conditions investigated. Under these restraints, the CDCC operated as desired. The top flow of the CDCC consisted primarily of ice crystals in suspension and the bottom flow of salt crystals in suspension.

Scaling of ice begins at the interface metal–fluid, with primary nucleation of ice. At the interface, not only the energy barrier for nucleation is the lowest due to the presence of the foreign, metallic surface, but also the supersaturation is the highest (lowest temperature). The nuclei subsequently grow to become crystals, forming an ice layer on the metallic surface that is not removed mechanically.

Scaling was first detected from a decreased heat transfer rate. If no measures were taken to revert the process, blockage of the scraper blades occurred. In experiments 2, 4 and 6 the scaling could be removed by quickly heating up the coolant to 313 K and then reestablishing the original temperature value. This operation took about 15 min and visually did not affect the ice and salt production. It can be assumed, however, that the steady state was disrupted. Usually, scaling manifested itself after about 7 h of operation, but the variability was significant: in experiments 7 and 8 no scaling was observed even after 13 h of operation. This variability in scaling behavior may be attributed to the primary nucleation step. It is a stochastic process that causes reproducibility problems in many crystallization processes.

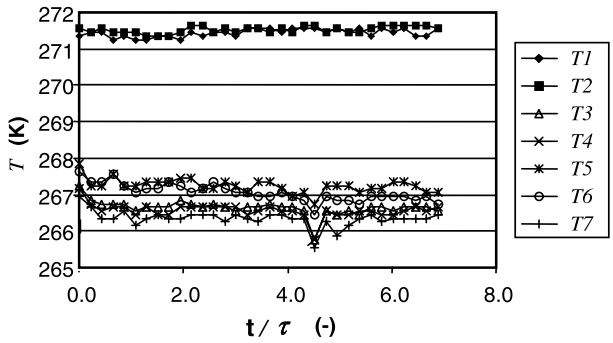


Fig. 7. Temperature levels in the CDCC for experiment 4 against crystallization time normalized with the residence time τ. T1 and T2 refer to suspension at the top and bottom; T3 and T4 to inlet cooling fluid; T5 and T6 to outlet cooling fluid; T7 is the temperature at the cooling bath. See sensor locations in Fig. 5.

Fig. 7 shows the temperature levels inside the CDCC for experiment 4 against the dimensionless time $t/\tau$, i.e. the time elapsed since initial formation of ice and salt divided by the residence time. The temperatures at the top and at the bottom of the crystallizer are similar and assume a constant value that is very close to the eutectic temperature (271.55 K). The data for all experiments show that the undercooling of the solution was within the range 0.05–0.4 K. The cooling fluid typically enters the crystallizer with a temperature 4.8 K lower than the suspension temperature and leaves it with a temperature 4.3 K lower, so the average temperature difference is 4.5 K. Taking into account all experiments, the range of temperature differences that allowed substantial production of ice and salt without scaling problems was 3.5–4.8 K.

The sudden decrease in the coolant temperature (channels 3–7) at $t/\tau = 4.5$ results from an overshoot of the cooling machine controller right after heating the cooling disks to remove scaling. The temperature of the bulk fluid inside the CDCC was not affected.

The heat flux transferred from the suspension to the cooling liquid was determined from measurements of the coolant flow and coolant temperatures. Fig. 8 shows that the heat flux for experiment 4 decreases slightly with time, probably due to ice crystals that are not removed by the scrapers. Average heat fluxes of all experiments as functions of the temperature difference across the cooling wall are depicted in Fig. 9. The slope of the curve has a value of 0.56 kW $m^{-2}$ $K^{-1}$, which represents the heat transfer coefficient $\alpha$ (Eq. (1)).

The heat flux calculated from measurements in the coolant was compared with calculations based on measurements on

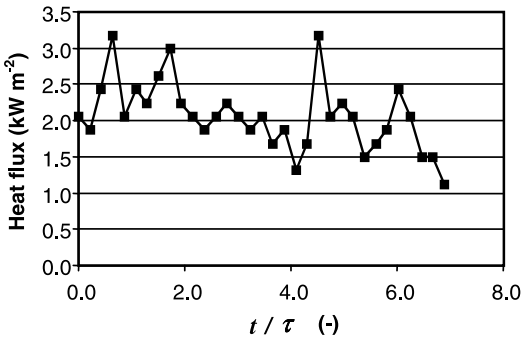


Fig. 8. Heat flux across the cooling disk surface for experiment 4 against the dimensionless time.

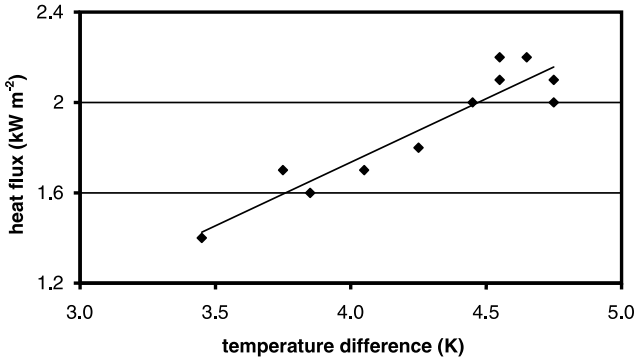


Fig. 9. Heat flux as a function of the temperature difference between cooling disk (average between inlet and outlet temperatures) and crystallizer.

the process streams for a normalized residence time $t/\tau$ of 6 (experiment 4). Table 2 shows the process mass flows and compositions involved. The heat fluxes so derived were, respectively, 2.1 and 1.5 kW m$^{-2}$. Since the error in the heat flux $\varepsilon(\phi''_H)$ for the former method of calculation, estimated from Eq. (8) for experiment 4, is 0.7 kW m$^{-2}$, the two methods for determination of the fluxes seem to be consistent.

### 4.2. Product quality

Both the ice and salt crystals are easily filtered. Optical micrographs of (unwashed) ice and salt crystals are shown in Figs. 10 and 11. Ice crystals are disk shaped with an average size of 150 μm. The salt crystals are equidimensional well faceted crystals, somewhat agglomerated, with an average size of 200 μm.

Table 2
Mass flows and compositions for experiment 4 at $t/\tau = 6.2$

| | | |
|---|---|---|
| $\dot{m}_{liq,top}$ | 67.5 | g min$^{-1}$ |
| $\dot{m}_{liq,bot}$ | 111.9 | g min$^{-1}$ |
| $\dot{m}_{ice}$ | 18.2 | g min$^{-1}$ |
| $\dot{m}_{salt}$ | 5.6 | g min$^{-1}$ |
| $x_{top}$ | 0.129 | – |
| $x_{bot}$ | 0.138 | – |
| $x_f$ | 0.140 | – |

Fig. 12 shows that the concentration of Cu in ice drops rapidly with repeated washing cycles. After three to four washing cycles, the concentration is below 100 ppm. If sufficient washing is applied, ice impurity content drops to 5 ppm or less. These results show that little copper is incorporated in the lattice structure of ice. Rather, most of the impurity in the ice is present in the washing liquor, either dissolved or in the form of entrained copper sulfate particles. The ice crystals were large enough for efficient washing, indicating that a future implementation of a CDCC followed by a filter or a wash column (see Section 2) may be successful in generating ice with only a few ppm of impurities.

### 4.3. Outlook for eutectic freeze crystallization

Application of EFC to different chemical systems brings specific requirements to ice and salt purity, as well as to allowed costs. Improved purity of the ice and salt crystals may be in principle obtained if crystallization is conducted at a low supersaturation. The resulting slow molecular growth rate contributes to low impurity incorporation, and the corresponding low nucleation rates lead to large crystals that are easily washed. In order to realize the crystallization under these conditions, a large heat transfer surface is needed, so that a trade-off between quality and cost is established.

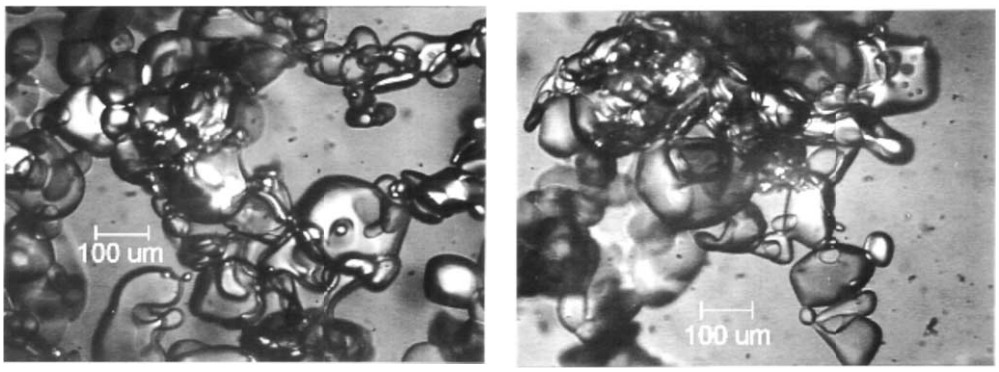


Fig. 10. Optical micrographs of ice crystals formed in the CDCC.

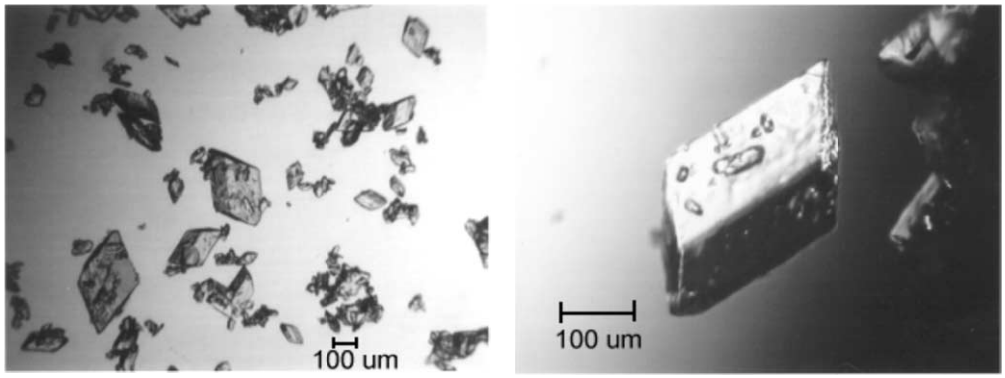


Fig. 11. Optical micrographs of $CuSO_4 \cdot 5H_2O$ crystals formed in the CDCC.

If a high purity is not required, higher supersaturations can be applied in order to obtain equipment that is more compact. However, a high supersaturation with respect to ice ($S_{ice}$) leads to excessive nucleation and growth upon the cooling surface, i.e. scaling. The allowed temperature difference across the heat transfer surface is system dependent, being in general larger for more impure systems. For a given temperature, a high surface area of ice crystals and a low surface area of salt also help prevent scaling by shifting the solution concentration (a more concentrated solution has a lower $S_{ice}$). For a given system, agitation of the bulk fluid breaks up and refreshes the stagnant boundary layer on the cooling surface, thereby contributing to minimize scaling.

Energy requirements for EFC of $NaNO_3$ and $CuSO_4 \cdot 5H_2O$ have been calculated to be, respectively, 30 and 65% of the energy needed in conventional three-step evaporation [4]. The eutectic temperatures for these systems were, respectively, 255 and 271 K. Here the technical feasibility for the copper sulfate system has been experimentally demonstrated. Preliminary laboratory scale results with a number of other salts (potassium phosphate, potassium sulfate and magnesium sulfate) indicate that no major technological barriers exist for EFC implementation. It is, therefore, reasonable to assume that EFC can be economically feasible to a large number of systems. However, for solutions with a low eutectic temperature, EFC may not be competitive with evaporative crystallization due to higher energy costs.

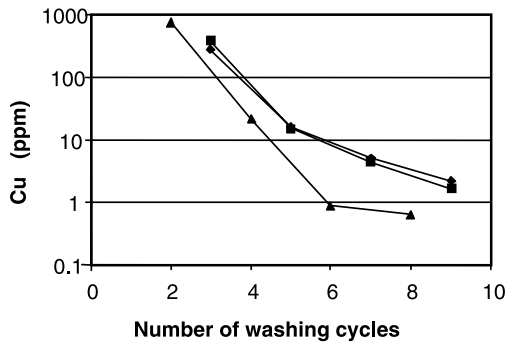


Fig. 12. Copper concentration in ice crystals against the number of washing cycles for three similar experiments.

## 5. Conclusions

A new type of equipment was introduced for EFC, the CDCC, which operates as a hybrid of crystallizer and solid/solid separator. Ice is formed and transported to the top of the column due to the lower density, whereas simultaneously crystallizing salt settles down. Top and bottom outlets are slurries of, respectively, ice and salt alone.

For crystallization of copper sulfate pentahydrate, the solution undercooling is less than 0.4 K with respect to the eutectic temperature. Excessive scaling upon the cooling disks occurs at a coolant temperature 4.8 K below the suspension temperature.

The newly designed CDCC produces 79 kg $h^{-1}$ $m^{-3}$ of ice and 21 kg $h^{-1}$ $m^{-3}$ of hydrated salt at a residence time of 1.7 h. The heat flux from the suspension to the cooling disk is 1.9 kW $m^{-2}$. Ice crystals formed in the CDCC show impurity levels below 5 ppm, are 150 μm in size and can be easily filtered and washed. The salt crystals are formed with sizes around 200 μm and can be easily filtered.

## Acknowledgements

The authors wish to thank NOVEM-The Netherlands Agency for Energy as well as the Ministry of Economic Affairs, the Ministry of Housing, Spatial Planning and Environment and the Ministry of Education and Science of the Netherlands through the EET program for their financial support.

## Appendix A. List of symbols

| | |
|---|---|
| $A_{cool}$ | area of cooling surface ($m^2$) |
| $C_p$ | specific heat (J $kg^{-1}$ $K^{-1}$) |
| $\dot{m}$ | mass flow rate (kg $s^{-1}$) |

| | |
|---|---|
| $N$ | number of cooling disks (−) |
| $R$ | ratio between top and bottom mass flow rates at the CDCC outlets (−) |
| $t$ | crystallization time (s) |
| $\bar{T}_{bulk}$, $\bar{T}_{disk}$ | temperatures in the bulk of the solution and in the cooling liquid (K) |
| $x$ | mass fraction (kg $CuSO_4$ in solution $kg^{-1}$ solution) |
| $x_{s,anh}$ | conversion factor (kg $CuSO_4$ $kg^{-1}$ $CuSO_4 \cdot 5H_2O$) |
| $\alpha$ | heat transfer coefficient (kW $K^{-1}$ $m^{-2}$) |
| $\Delta H_{crys}$ | heat of crystallization (kJ $kg^{-1}$) |
| $\varepsilon(T)$ | error in temperature measurement (K) |
| $\varepsilon(\phi_H)$ | error in heat flow determination (kW) |
| $\phi_H$ | heat flow between cooling disk and bulk fluid (kW) |
| $\phi''_H$ | heat flux between cooling disk and bulk fluid (kW $m^{-2}$) |
| $\tau$ | residence time in the crystallizer (s) |

*Subscripts*

| | |
|---|---|
| *bot, top* | bottom and top outlets of the crystallizer |
| *cool* | cooling liquid |
| *D*1, *D*2. . . | cooling disk 1, 2 . . . |
| *feed* | feed |
| *liq* | liquid phase |
| *salt, ice* | solid $CuSO_4 \cdot 5H_2O$ and water |

## References


[1] F. van der Ham, G.J. Witkamp, J. de Graauw, G.M. van Rosmalen, Eutectic freeze crystallization simultaneous formation and separation of two solid phases, J. Cryst. Growth 198–199 (Part 1) (1999) 744–748.

[2] G.L. Stepakoff, D. Siegelman, R. Johnson, W. Gibson, Development of a eutectic freezing process for brine disposal, Desalination 14 (1974) 25–38.

[3] A.J. Barduhn, A. Manudhane, Temperatures required for eutectic freezing of natural waters, Desalination 28 (1979) 233–241.

[4] F. van der Ham, G.J. Witkamp, J. de Graauw, G.M. van Rosmalen, Eutectic freeze crystallization: application to process streams and waste water purification, Chem. Eng. Process 37 (1998) 207–213.

[5] G.F. Arkenbout, Melt Crystallization Technology, Technomic Pub. Co, Lancaster, PA, 1995.

[6] P.J. Diepen, Cooling crystallization of organic compounds, Ph.D. thesis, Delft University of Technology, Delft University Press, Delft, The Netherlands, 1998.